

1
2
3
4
5
6
7
8
9
10
11
12
13
14
15
16
17
18
19
20
21
22
23
24

**Characterization of Soil Moisture Response Patterns and Hillslope Hydrological Processes
through a Self-Organizing Map**

Eunhyung Lee¹, Sanghyun Kim¹

¹Department of Environmental Engineering, College of Engineering, Pusan National University, Busan,
South Korea

Corresponding author: Sanghyun Kim (kimsangh@pusan.ac.kr)

Key Points:

A hydrologic dataset can be classified and characterized by applying a machine learning algorithm.

The self-organizing map is useful to understand the soil moisture response pattern at a hillslope
scale.

Five event clusters distinctively represent different combinations of hydrological processes.

메모 포함[오전1]: Addressing comment for reviewer 2 for title

메모 포함[오전2]: Key points were revised to address reviewer 2's point.

25 **Abstract**

26 Hydrologic events can be characterized as particular combinations of hydrological processes on a
27 hillslope scale. To configure hydrological mechanisms, we analyzed a dataset using an
28 unsupervised machine learning algorithm to cluster the hydrologic events based on the
29 dissimilarity distances between the weighting components of a self-organizing map (SOM). The
30 time series of soil moisture was measured at 30 points (at 10 locations with three different depths)
31 for 356 rainfall events on a steep, forested hillslope between 2007 and 2016. The soil moisture
32 features for hydrologic events can be effectively represented by the antecedent soil moisture, soil
33 moisture difference index, and standard deviation of the peak-to-peak time between rainfall and
34 soil moisture response. Five clusters were delineated for hydrologically meaningful event
35 classifications in the SOM representation. The two-dimensional spatial weighting patterns in the
36 SOM provided more insights into the relationships between rainfall characteristics, antecedent
37 wetness, and soil moisture response at different locations and depths. The distinction of the
38 classified events could be explained by several rainfall features and antecedent soil moisture
39 conditions that resulted in different patterns attributable to combinations of hillslope hydrological
40 processes, vertical flow, and lateral flow along either surface or subsurface boundaries for the
41 upslope and downslope areas.

42

43 **Keywords:** rainfall, soil moisture, hillslope hydrology, self-organizing map, process-based
44 characterization

45

46

47

48

49 **1 Introduction**

50 Soil moisture information is critical for assessing water storage, for estimating the quantity of
51 runoff generated, and for determining the slope stability of hillslopes during rainfall (Angermann
52 et al., 2017; Lu and Godt, 2008; Penna et al., 2011; Tromp Van Meerveld and McDonnell, 2005).

53 Hillslope hydrological processes are affected by several factors, including topography, soil texture,
54 and eco-hydrological parameters (Baroni et al., 2013; Liang et al., 2011; Rodriguez-Iturbe et al.,
55 2006; Rosenbaum et al., 2012; Western et al., 1999), which result in highly nonstationary and
56 heterogeneous spatiotemporal distributions of soil moisture (Penna et al., 2009; Wilson et al.,
57 2004). The relationship between precipitation and runoff is highly nonlinear, and the
58 spatiotemporal variations in soil moisture, groundwater, and surface runoff cannot be easily
59 predicted (Ali et al., 2013; Curtu et al., 2014).

60 Rainfall is the primary driver of rapid variations in soil moisture and subsurface flow
61 generation (Penna et al., 2011). The response of soil moisture to rainfall events has been
62 investigated for various topographic positions, depth profiles, and land cover conditions (Feng and
63 Liu, 2015; He et al., 2012; Wang et al., 2013; Zhu et al., 2014). The functional relationship between
64 rainfall events and soil moisture depends on several factors, such as soil texture, depth, topography,
65 and vegetation cover (Bachmair et al., 2012; Gwak and Kim, 2016; Liang et al., 2011). Rainfall
66 characteristics, including the total quantity, duration, intensity, and dry period duration, have also
67 been explored to understand the soil moisture response (Albertson and Kiely, 2001; Heisler-White
68 et al., 2008). Other studies conducted on rainfall features have reported the categorization of
69 rainfall events to analyze soil moisture variation (Lai et al., 2016; Wang et al., 2008).

70 Antecedent soil moisture (ASM) plays an essential role in the hydrological response at the
71 hillslope scale (Hardie et al., 2011; Lee and Kim, 2020; Uber et al., 2018). The interaction between
72 the spatial distribution of ASM and rainfall events determines various hydrological processes, such
73 as the occurrence of preferential flow, soil moisture variation patterns, subsurface stormflow, and
74 runoff generation (Bachmair et al., 2012; Saffarpour et al., 2016; Wiekenkamp et al., 2016; Zhang
75 et al., 2011). The wetter ASM and the greater rainfall events resulted in a higher variation in soil
76 moisture and deeper rainwater percolation (Lai et al., 2016; Lee and Kim 2020; Zhu et al., 2014).
77 Owing to the generation of distinct hillslope flow paths, vertical flows (either matrix or bypass
78 flows) and lateral flows along different boundaries (e.g., subsurface stormflow over bedrock and
79 surface overland flow) can vary along a transect of the hillslope (Wienhöfer and Zehe, 2014).
80 Previous studies have investigated the functional relationship between rainfall and soil water
81 storage (Castillo et al., 2003; Crow and Ryu, 2009; Trambly et al., 2012). However, the influence
82 of rainfall features such as rainfall amount, intensity, duration, and ASM conditions on the
83 generation of hillslope flow paths and their distributions at the hillslope scale have not been
84 sufficiently explored. Other studies on hillslope hydrology have focused on several events to
85 identify specific flow paths (e.g., subsurface lateral flow) using intensively collected field
86 measurements over relatively short periods (Freer et al., 2004; Kim 2009; Penna et al., 2011;
87 Wienhöfer and Zehe, 2014).

88 A comprehensive approach can be useful for addressing the holistic behavior of
89 hydrological processes using a dataset of a substantial number of events collected over several
90 years. Identification of specific hydrological processes through visual inspection of field data can
91 be labor-intensive, and the accuracy of analysis can be marginal and subjective if the size of the
92 dataset is not substantial.

93 Machine learning techniques have been applied to soil moisture data derived from in situ
94 measurements (Van Arkel and Kaleita, 2014; Carranza et al., 2021; Ley et al., 2011), remote
95 sensing applications (Ahmad et al., 2010; Srivastava et al., 2013), and from the analysis of
96 hydrological model performance (Herbst et al., 2009; Shrestha et al., 2009). Supervised learning
97 algorithms have been used to improve predictions of subsurface flow in a hillslope (Bachmair et
98 al., 2012), to downscale satellite soil moisture data (Srivastava et al., 2013), and to estimate the
99 soil moisture obtained through regression analysis (Ahmad et al., 2010). Critical soil moisture
100 sampling points have also been identified using unsupervised learning algorithms (Liao et al., 2017;
101 Van Arkel and Kaleita, 2014). Most studies involving machine learning algorithms for the analysis
102 of soil moisture have focused on the estimation and determination of the appropriate measurement
103 locations for the assessment of variations in mean soil moisture. However, the soil moisture
104 response can be further explored in the context of hydro-meteorological (rainfall), hydro-historic
105 (ASM), and topographic (location and depth) controllers at the hillslope scale.

106 A self-organizing map (SOM), which is an unsupervised neural network method, has been
107 used to investigate datasets representing ecosystems, animals, catchment classification, and crop
108 evapotranspiration (Casper et al., 2012; Farsadnia et al., 2014; Ismail et al., 2012; Ley et al., 2011).
109 The SOM can be considered an effective tool for understanding substantial hydrologic data by
110 reducing the dimensionality of a dataset, which can help provide hydrologic interpretation
111 (Reusser et al., 2009). Furthermore, an SOM can be used to successfully address the nonlinear
112 relationship between hydrologic variables (Chen et al., 2018; di Prinzio et al., 2011; Ley et al.,
113 2011; Toth, 2013). The highly heterogeneous and extremely nonstationary variation in soil
114 moisture between the upslope and downslope areas alongside the upper, middle, and lower soil

메모 포함[오전3]: Addressing reviewer' s point for another reference of SOM.

115 layers of a hillslope can be analyzed using an SOM. We aimed to answer the following research
116 questions:

- 117 1. How can machine learning algorithms be used to understand the soil moisture response
118 patterns at the hillslope scale?
- 119 2. Can delineated clusters of hydrologic events be explained by different hillslope
120 hydrological processes?

121 In the present study, an alternative method for understanding hillslope hydrologic behavior
122 was explored through long-term data analysis using SOM. Hydrologic events for the hillslope scale
123 can be characterized through a rigorous classification of a substantial hydrologic dataset. The
124 application of machine learning algorithms provides several opportunities for understanding
125 hydrologic events by transforming a substantial dataset into compact clusters and by delineating
126 the hierarchical relationship between clusters, which can be useful for exploring process-based
127 interpretations and for obtaining an efficient monitoring network. We used hydrologic data
128 (rainfall and soil moisture) to analyze and characterize the highly complex relationships between
129 ASM, rainfall characteristics, and soil moisture responses, which included variations in soil
130 moisture and the time to peak. The SOM was used to investigate the nonlinear interactions between
131 various rainfall characteristics and their effects on temporal changes in soil moisture and to classify
132 the multivariate datasets regarding the likely flow paths in the hillslope.

133 We used the following approaches to address these research topics: first, we applied an
134 SOM algorithm to datasets composed of rainfall features, ASM, and soil moisture status from
135 upslope to downslope locations in the study area. The dataset was reclassified based on the
136 weighting vectors of each neuron in the SOM map using the Euclidean distances between distinct
137 hydrological variables from individual hydrologic events. Second, the nonlinear relationship

138 between rainfall and soil moisture was evaluated by comparing spatially weighted patterns of
139 rainfall characteristics and soil wetness variables. The relationships between rainfall characteristics
140 and soil moisture at varying depths and locations were investigated, and these data were used to
141 interpret the hydrological processes.

142

143 **2 Materials and Methods**

144 **2.1 Study area and data acquisition**

145 The hillslope (area, 4000 m²) selected for the study is in the Sulmachun watershed (area: 8.5 km²),
146 which is considered the headwater of the Imjin River in northwestern South Korea (Fig. 1). The
147 study area is primarily covered by a mixture of *Polemoniales*, shrubby *Quercus*, and a coniferous
148 canopy of *Pinus densiflora*, with slopes varying between 30° and 45°. Data on rainfall, streamflow,
149 and other hydrometeorological records (e.g., temperature and relative humidity) have been
150 collected over the last 25 years from seven hydrologic monitoring stations in this watershed (Fig.
151 1). The mean annual rainfall for the last two decades was approximately 1,500 mm; 70% of the
152 total rainfall occurred during the Asian monsoon season between June and August. Precipitation
153 in the form of snowfall occurred between December and March. The mean annual evaporation was
154 approximately 420 mm and was estimated using the eddy-covariance method with data obtained
155 from a flux tower (adjacent hydrologic monitoring station) located 50 m away from the study area.
156 The average daily temperature varied between -15°C and 35°C. The hillslope bedrock consists of
157 granite with extensively weathered areas. Elevations range between 200 and 260 m above sea level,
158 and the surface slope varies between 20° and 35°. Leptosols and Cambisols (classifications
159 according to the Food and Agricultural Organization of the United Nations) are the dominant soils
160 in the upslope and downslope areas, respectively. Analysis of 15 soil samples (based on the

161 consideration of 5 points each from the upslope and downslope areas at depths of 30 cm) indicated
162 that the predominant soil textures were sandy loam and loamy sand. The average porosities for the
163 upslope and downslope areas were 49% and 48%, respectively. Multiple insertions of an iron pole
164 at each grid cell (0.5 × 0.5 m) indicated that the soil depth along the hillslope varied between 25
165 and 95 cm. The depth of the root zone was approximately 20–30 cm.

166 Rainfall data (used to describe rainfall characteristics) were recorded at hourly intervals
167 using a rainfall gauge (automatic rain gauge system, Eijkelkamp) placed under the canopy. The
168 soil moisture time series were assessed using a multiplex-based time domain reflectometer (TDR;
169 MiniTRASE, SoilMoisture, 2004) at five locations each for upslope (UP1–UP5) and downslope
170 areas (DO1–DO5) (Fig. 1). At each location, three TDR sensors (waveguides) were inserted
171 parallel to the surface at depths of 10, 30, and 60 cm into the upslope side of the installation trench
172 that was filled with soil. Soil moisture measurements were collected hourly between 2007 and
173 2016. There were 356 rainfall events documented during the study period. A rainfall event was
174 defined as a minimum dry period of 1 d and a minimum of 1 mm of rainfall.

175

176 **2.2 Data analysis for soil moisture response**

177 For a given rainfall event, the variation in soil moisture at a particular point in the hillslope depends
178 not only on the rainfall but also on other environmental factors such as the location, depth, and soil
179 texture. To consider the relative variation (%) of water storage normalized by the ASM condition,
180 we used the soil moisture difference index, which is defined as the percentage of maximum soil
181 moisture difference (Zhu et al., 2014), to represent the soil moisture variation as follows:

$$182 \quad \Delta\theta(\%) = \frac{\theta_{max} - \theta_{ant}}{\theta_{ant}} \times 100, \quad (1)$$

183 where θ_{max} represents the maximum soil moisture during a rainfall event and the subsequent
184 period (≤ 4 h), and θ_{ant} represents the soil moisture measurement before the rainfall event (2 h).

185 We also calculated the time from peak to peak (P2P, in h), which is defined as the time difference
186 between the peak of rainfall and the maximum soil moisture variation. The standard deviation of
187 P2P (SDP2P) for the measuring points was used to represent the homogeneity of the soil moisture
188 responses (Kim, 2009). The time series information of the soil moisture was converted to address
189 distinct response features for rainfall events. Depending on the soil moisture responses in the
190 transect, location, and depth, 12 different soil moisture response features were delineated as
191 follows: behavior of all measurements (total); measurements at upslope points (upslope); and those
192 for downslope (downslope); measurements at depths of 10 cm (10 cm), 30 cm (30 cm), and 60 cm
193 (60 cm); measurements for upslope at depths of 10 cm (UP10 cm), 30 cm (UP30 cm), and 60 cm
194 (UP60 cm); and measurements for downslope at depths of 10 cm (DO10 cm), 30 cm (DO30 cm),
195 and 60 cm (DO60 cm).

196

197 **2.3 Unsupervised machine learning algorithm**

198 The SOM utilizes an unsupervised learning algorithm that can be useful for pattern recognition of
199 multivariate datasets from different observations. The SOM is typically a two-dimensional (2D)
200 grid composed of either hexagonal or rectangular elements. In this study, we used a hexagonal
201 lattice as the output layer because it resulted in better information propagation when updating more
202 neighborhood neurons than those of the rectangular lattice (Kohonen, 2001).

203 Input variables for the SOM computation were obtained from rainfall features such as
204 rainfall duration (DUR), rainfall amount (AMO), rainfall intensity (INT), ASM, soil moisture
205 difference index and SDP2P for upslope areas at depths of 10, 30, and 60 cm, and those for the

206 downslope area at depths of 10, 30, and 60 cm, respectively. A log transformation was applied to
207 all input variables to fit the bounds of data between zero and one, except SDP2P, which was <1 in
208 most cases.

209 SOM maps were established for each variable, and the distance between the input vector
210 and weighting vector could be calculated as follows:

$$211 \quad d_b = \sqrt{\sum_{a=1}^v (w_{a,b} - x_a)^2}, \quad (2)$$

212 where v represents the number of variables.

213 The best neuron can be identified as the neuron with the minimum value of d_b indicating
214 the best fitness to the characteristics of each rainfall event among every neuron in the SOM. Once
215 the neuron is selected, the weighting vector should be re-evaluated using Eq. 3 for the renewal
216 weighting vector expressed as follows:

$$217 \quad \Delta w_{a,b} = \begin{cases} \alpha(x_a - w_{a,b}) & b = b^* \\ 0 & b \neq b^* \end{cases}$$
$$w_{a,b}^{new} = w_{a,b}^{old} + \Delta w_{a,b}, \quad (3)$$

218 where α ($= 0.5$) represents the acceleration coefficient, and b^* represents the winner neuron.

219 After updating the algorithm, all neurons in the SOM maps fit weighting vectors to the
220 multiple datasets used in this study. The input variables in each neuron can be displayed in the
221 component planes, and these are depicted as spatial patterns in SOM maps. The nonlinear
222 relationship between variables was identified through visual comparison between the spatially
223 distributed weightings in each component plane (Adeloye et al., 2011; Farsadnia et al., 2014;
224 García and González, 2004; Park et al., 2003).

225

226 **2.4 Clustering of hydrologic events**

227 Clusters within the dataset can be delineated by applying the dendrogram classification method
228 and by evaluating the dissimilarity between the weighting vectors (Montero and Vilar, 2014). The
229 Euclidean distance function was considered to evaluate the dissimilarity, as it is suitable for
230 deducing shape-based comparisons between soil moisture series whose data are collected
231 simultaneously (Iglesias and Kastner, 2013). This method has also been used to identify clusters
232 of soil moisture data (Van Arkel and Kaleita, 2014). The Euclidean distance between two
233 weighting vectors in neurons (b_1 and b_2) can be expressed as follows:

234
$$d_{b_1 b_2} = [\sum_{a=1}^v (w_{a,b_1} - w_{a,b_2})^2]^{0.5}. \quad (4)$$

235 The relationship that exhibits the shortest distance between neurons is assigned to the first cluster,
236 and the weighting vectors of the first cluster can be expressed as:

237
$$\mu_{c_1, a} = \frac{n_{b_1} \mu_{b_1} + n_{b_2} \mu_{b_2}}{n_{b_1} + n_{b_2}}, \quad (5)$$

238 where μ_{b_1} and μ_{b_2} represent the variable weighting vectors in the neurons (b_1 and b_2), respectively;
239 n_{b_1} and n_{b_2} are set to a value of 1 in this relationship, but these values are set to the number of
240 components during the comparison of clusters. Additionally, we used Ward's method to evaluate
241 the dissimilarity between two weighting vectors of each neuron, and between each cluster, i.e., this
242 was the chosen algorithm in our hierarchical clustering method (Ward, 1963). When the
243 dissimilarity between two clusters (c_1 and c_2) is calculated, the distance between clusters can be
244 expressed as:

245
$$d_{cluster} = \sum_{a=1}^v \frac{\|\mu_{a,c_1} - \mu_{a,c_2}\|^2}{\frac{1}{n_{c_1}} + \frac{1}{n_{c_2}}}, \quad (6)$$

246 where μ_{a,c_1} and μ_{a,c_2} represent the averages of clusters c_1 and c_2 , respectively, and n_{c_1} and n_{c_2}
247 represent the numbers of components for clusters c_1 and c_2 , respectively. A dendrogram can be
248 constructed based on the resulting $d_{cluster}$, and the upper part from a designated horizontal line
249 can be recognized as the structure of the final clusters.

250

251 **3 Results**

252 **3.1 Soil moisture responses of all measuring points during rainfall events**

253 The statistics of soil moisture response based on the analysis of 30 points are summarized in terms
254 of the P2P and maximum variation, as displayed in Fig. 2(a) - 2(f), which present elevations as an
255 order of locations in x-axis as UP1-UP4-UP2-UP5-UP3-DO1-DO2-DO3-DO4-DO5 (Fig. 1) from
256 the hilltop to downslope. The means of P2P ranged from -0.2 d to $+0.5$ d, indicating that the
257 maximum soil moisture could be achieved even before the occurrence of the rainfall peak. Both
258 standard deviation and average of P2P tended to increase at deeper depths, except for locations
259 with elevations in 224 m and 216 m (locations of DO2 and DO5 in Fig. 1).

260 Fig. 2(a), 2(c) and 2(e) indicate while the mean P2P for the upslope area was 0.24 d, that of the
261 downslope area was 0.02 d. The mean values of P2P at depths of 10, 30, and 60 cm were -0.08 ,
262 0.04, and 0.011 days for the downslope and were 0.1, 0.24, and 0.38 days for upslope, respectively.

263 The differences in P2P between other points at an identical depth for the downslope were smaller
264 than those for the upslope. This suggests that the soil moisture response in the downslope area is
265 faster and more uniform than that in the upslope area. The accumulated soil water flow from the
266 upslope area to the downslope area seems to be responsible for more rapid and less spatially
267 variable soil moisture responses in the downslope area. As shown in Figs. 2(b), 2(d) and 2(e), both
268 average and standard deviation of maximum variation tend to increase for locations with lower

269 elevation. The average of maximum variations at depths of 10 cm and 60 cm were higher than
270 those for the 30-cm depth, indicating that primary lateral flow tended to be generated along
271 boundaries (surface and subsurface).

272

273 3.2 Soil moisture response features in measuring locations and depths

274 The soil moisture response features (e.g., ASM, soil moisture difference index, and SDP2P) were
275 expressed in different spatially averaged responses (Fig. 3), depending on the depth and location.

276 As shown in Fig. 3(a), the ASM in the downslope area was higher than that in the upslope area. It
277 was apparent that the ASM in the downslope area increased with increasing depth; however, ASM
278 for the upslope area did not display any notable trend in the depth profile. This indicated that soil
279 water infiltration in the upslope area did not necessarily occur for all depth profiles.

280 The soil moisture difference index in the downslope area was higher than that in the upslope area,
281 as shown in Fig. 3(b). The average soil moisture difference index in the downslope area (50.67%)
282 was higher than that of the upslope area (38.73%), and the average soil moisture difference indices
283 at depths of 10, 30, and 60 cm for the upslope area were 44.51%, 34.27%, and 37.39%, while those
284 for the downslope area were 64.49%, 40.83%, and 46.69%, respectively. This indicates higher
285 wetness along both the surface and subsurface boundaries, and this trend is pronounced in the
286 downslope direction.

287 The SDP2Ps for the soil moisture datasets represent the degree of spatial heterogeneity in the
288 temporal soil moisture response. The statistics of the SDP2P (Fig. 3(c)) revealed that the
289 downslope response varied less than the upslope response. While the SDP2P of the downslope
290 displayed an apparent increasing trend at deeper depths, those for the upslope showed a similar in-
291 depth profile. The difference in the SDP2P profile between the upslope and downslope indicates

메모 포함[오전4]: Revised context for comment "Fig.2 is better to present boxplots not using the profile names but their topographical elevation on the x-axis (more information), and it might be better to separate different depths into different panels"

Addressing comment 1 from reviewer 2
-Figure 2 and Figure 3 were revised to improve readability (simple way) and corresponding explanations were added.

292 that the impact of rainfall on soil moisture response timing can be completely different between
293 the upslope and downslope directions.

294 The relationships of each response feature (e.g., ASM, Soil moisture difference index, and SDP2P)
295 among different soil moisture datasets can be visualized through the heat map presented in Fig. 4.
296 As displayed in Fig. 4, the heat maps for ASM ranged from 0.88 to 0.99, and those for soil moisture
297 difference indices and SDP2P ranged from 0.78 to 0.98 and from 0.40 to 0.90, respectively. The
298 relationship between upslope and downslope (${}_2C_2$; i.e., the first combination), those between
299 identical depths (${}_3C_2$; i.e., the second combination), and those for different depths and locations
300 (${}_6C_2$; i.e., the third combination) indicate the heterogeneity of different soil moisture features in
301 the spatial context. The values for the first combination for ASM, soil moisture difference index,
302 and SDP2P were 0.81, 0.72, and 0.53; the mean values of second and third combinations were
303 0.95, 0.84, and 0.62, and 0.83, 0.69, and 0.35 for ASM, soil moisture difference indices, and
304 SDP2P, respectively. This suggested that the spatial distribution of ASM did not demonstrate
305 meaningful spatial variability, but those for soil moisture difference indices and SDP2P were
306 substantial. Therefore, soil moisture difference index and SDP2P can be deemed useful variables
307 for the characterization of the spatial variation of the soil moisture response for the application of
308 SOM.

309

310 **3.3 Composition and clustering of SOM**

311 The dataset of hydrologic measurements (356×15) was transformed through the application of
312 96 neurons and output based on a matrix (16×6) through the iterative application of Eqs. (5) and
313 (6), respectively, i.e., 15 hydrologic variables derived from 356 events were expressed in a
314 compact manner in the SOM. Many alternatives exist in the number of clusters, depending on the

메모 포함[오전5]: Addressing comment 1 from reviewer
2
Figure 2 and Figure 3 were revised to improve
readability (simple way) and corresponding
explanations were added.

315 complexity of the dendrogram structure. In this study, five clusters were selected based on a
316 heuristic approach to achieve a hydrologically meaningful classification of events and
317 parsimonious clustering. The relation to notable hydrological processes such as lateral flow or
318 vertical preferential flow and the redundancy check in cluster number were essential factors in the
319 implementation of the heuristic approach. Figure 5(a) illustrates the resulting dendrogram for the
320 five clusters. The structure of the dendrogram demonstrates the relationships between groups of
321 clusters and between individual clusters. Figure 5(b) presents the output SOM (16×6) delineated
322 from the dendrogram analysis, which is a structural array identical to the delineated dendrogram
323 with neurons for each cluster. The spatial distributions between other clusters and the
324 corresponding numbers of neurons indicate the areal portion of each cluster from all clusters and
325 their connections with adjacent clusters.

326 Table 1 presents the average of vector components, such as the AMO, DUR, INT, and
327 average ASM among all measuring points (ASMTOT) in volumetric %, along with an average of
328 the soil moisture difference indices ($\Delta\theta$) in five upslope locations and five downslope locations at
329 depths of 10, 30, and 60 cm, as VUP10, VUP30, VUP60, VDO10, VDO30, and VDO60.
330 Additionally, it presents the SDP2P in five upslope and five downslope locations at depths of 10,
331 30, and 60 cm, as SUP10, SUP30, SUP60, SDO10, SDO30, and SDO60, respectively, for the five
332 clusters displayed in Fig. 5(b).

333 As displayed in Fig. 5(b), Clusters 1 and 2 were located in the upper part of the SOM. Table
334 1 indicates that the rainfall characteristics of Clusters 1 and 2, such as DUR, AMO, and INT, were
335 relatively low, but those for the ASM were similar to the mean ASM for all clusters (Table 1). The
336 average soil moisture difference indices were less than 5% for Cluster 1 because the low AMO
337 and intensity resulted in a limited increase in soil water storage, and the loss due to evaporation

338 offset a substantial proportion of the precipitation (Albertson and Kiely, 2001; Ramirez et al.,
339 2007). Cluster 2 exhibited higher AMO and intensities and more significant average soil moisture
340 differences indices than Cluster 1 (Table 1). The intermediate part of the SOM (Fig. 5(b)) was
341 associated with Cluster 3, which revealed higher rainfall durations, quantities, and intensities than
342 those for Clusters 1 and 2, which resulted in higher soil moisture difference index for Cluster 3
343 than those for Clusters 1 and 2 (Table 1). One notable feature of Cluster 3 was the increasing trend
344 of soil moisture difference indices with depth ($DO_{60} > DO_{30}$) for the downslope area, whereas
345 those of Clusters 1 and 2 displayed decreased soil moisture difference indices with depth (DO_{30}
346 $> DO_{60}$) (Table 1). The pattern of soil moisture difference index for Cluster 3 suggests vertical
347 infiltration in all depth profiles for upslope and apparent lateral flow for downslope areas (Table 1
348 and Fig. 4), which seems to be completely different from those for Clusters 1 and 2. Clusters 4 and
349 5 demonstrated a greater soil moisture difference index, with significant events in the SOM
350 classification (Table 1). Cluster 4 displayed two distinctive features compared to other clusters.
351 Firstly, the ASM of Cluster 4 was the lowest among all clusters. However, the soil moisture
352 difference indices at depths of 30 and 60 cm in the downslope area for Cluster 4 were significantly
353 higher than those in Clusters 1, 2, and 3. Secondly, the difference in VAR between the upslope
354 and downslope areas was the most pronounced in Cluster 4. This suggests that the hydrological
355 processes in the upslope and downslope areas can be substantially distinct from each other. Both
356 rainfall characteristics and soil moisture difference index for Cluster 5 were significantly higher
357 than those for all other clusters. Several measurement data points in Cluster 5 exhibited saturation
358 during rainfall events, and the soil moisture at a depth of 60 cm displayed higher variation than
359 that at 30 cm, which indicated that subsurface stormflow was generated along the bedrock in both
360 the upslope and downslope areas.

361 The centroid for each cluster was calculated by averaging combinations of weighting
362 vectors in the neurons. The event having the smallest root mean squared error between input
363 variables of each event and the centroid of each cluster was selected as the exemplary event for
364 corresponding cluster. Appendix presents exemplary events with rainfall and soil moisture
365 responses at several upslope and downslope points for Clusters 1 to 5. The exemplary event for
366 Cluster 1 showed almost no response to rainfall and that of Cluster 2 resulted into limited responses
367 in designated downslope locations. Both events from Cluster 3 and 4 showed apparent response in
368 many points with a difference in lower antecedent soil moisture condition for Cluster 4. The
369 exemplary event for cluster 5 showed significant recharge impact in soil moisture for most points.

메모 포함[오전6]: 1.Response for final reviewer's comment for "Another option would be to show the events closed to the cluster centroids."

371 3.4 Component planes for variables

372 Information on the component planes of 16 variables and their visual comparisons can help provide
373 insights into the nonlinear relationships between the 16 hydrological variables. Figure 6 illustrates
374 the SOM distributions for the component weightings of the 16 variables. Both the spatial
375 distributions and the scales of weightings (scale bar) in Fig. 6 represent the characteristics of
376 impacts (rainfall features and ASM) and consequences (average of soil moisture difference and
377 SDP2P).

378 The visual comparison of Fig. 6(a)–6(d) indicates a negligible relationship between rainfall
379 features and ASM. The component planes for upslope soil moisture difference indices at depths of
380 10, 30, and 60 cm (Fig. 6(e)–6(g)) displayed similar spatial weightings to those for rainfall features.
381 The high weightings for the soil moisture difference index at a 10-cm depth were mainly
382 distributed to Clusters 4 and 5, and the weightings tended to concentrate in Cluster 5 at higher

383 values of depths (Fig. 5). The comparison between ASM and soil moisture differences index
384 indicated that ASM did not influence the soil moisture differences index.

385 The exclusive vertical flow impact can be proposed as one possible explanation for the
386 relationship between the component plane for VUP10 and those for VUP30 or VUP60 (Fig. 6(e),
387 6(f), and 6(g)), because there were negligible contributing areas or small values of topographic
388 wetness indices (Fig. 1) in upslope locations. Weightings in VUP10 were associated with AMO
389 and INT, but those for VUP60 correlated only with AMO. This pattern of weighting shift was
390 observed between VUP30 and VUP60, which could be attributed to the effect of vertical
391 infiltration (Li et al., 2013). This relationship along the vertical profile differed between the
392 upslope and downslope. The development of the vertical gradient in weightings (Fig. 6(e)–6(g))
393 from VUP10 to VUP60 can barely be observed in weightings from VDO10 to VDO60 (Fig. 6(h)–
394 6(j)). This suggests that the flow path in the downslope area cannot be completely explained by
395 the vertical flow.

396 Figures 6(k)–6(m) display the component planes of SDP2P at depths of 10, 30, and 60 cm
397 in the upslope area. The weighting distributions between upslope SDP2P (Fig. 6(k)–6(m)) and
398 ASM (Fig. 6(d)) were completely reversed. The spatial distribution of SDP2P in the downslope
399 did not reveal a notable difference in the in-depth profile (Fig. 6(n)–6(p)). This could be explained
400 by the possibility that the time to peak in the downslope was not only determined by rainfall but
401 was more affected by other drivers such as topography.

402

403 **4 Discussion**

404 **4.1 Characterization of the classified hydrologic events**

405 The hydrologic events classified by the SOM can be characterized through a comparative feature
406 presentation for all clusters (Fig. 7). The lower ASM matched with a higher mean and wider bound
407 in SDP2P, which could also be confirmed by the component planes of ASM and SDP2P. With
408 increasing depth, the heterogeneity in response time increased (greater SDP2P) in most locations.
409 This can be explained by the response time between rainfall and soil moisture decreasing with
410 depth. The SDP2P response between the upslope and downslope can be distinctly expressed
411 depending on the cluster. Clusters 1 and 2 exhibited negligible differences in hillslope transects,
412 but those for Clusters 3, 4, and 5 were substantially different. This is because the generation of
413 lateral flow can be more significant under greater rainfall events in downslope than that in upslope
414 areas. The soil moisture peak formations matched well with the soil moisture difference indices in
415 soil moisture at the downslope. Events in Cluster 1 demonstrated less variation in SDP2P for both
416 depth profile and hillslope transect location because of the lowest AMO and INT values. The
417 impact of depth on the variation of SDP2P can be observed in Clusters 2, 3, and 5, and with
418 increasing depth, the bound was higher in both upslope and downslope areas. However, this pattern
419 was different between the upslope and downslope in Cluster 4 that presented with the lowest ASM.
420 The lowest ASM led to substantially less response variation at a 60-cm depth in the upslope, while
421 that for the downslope revealed higher variation at a 60-cm depth compared to that reported at
422 shallower depths. This suggested that the dominant flow path between the upslope and downslope
423 was different in Cluster 4.

424 The increasing pattern of the soil moisture difference indices corresponds to increasing
425 rainfall features such as DUR and INT from Clusters 1 to 5. However, the depth profile of the soil
426 moisture difference index differed between Clusters 4 and 5. While the scale of soil moisture
427 recharge demonstrated an apparent decrease in the depth profile for Cluster 4, that for Cluster 5

메모 포함[오전기]: Fig. 7 is cited for comment from reviewer
1

428 demonstrated different surface and subsurface boundaries (at depths of 10 and 60 cm). This
429 indicated that the dominant hydrological processes for Cluster 4 appear restricted to the surface as
430 the vertical flow, but those for Cluster 5 existed at both the surface and subsurface boundaries as
431 both vertical and lateral flows.

432 The impact of rainfall events on water storage can be useful for understanding the changes
433 in various hydrological statuses for each cluster. The storage changes (Table 2) were estimated by
434 multiplying the soil moisture change by the corresponding depth for each waveguide (e.g., 200
435 mm for 10 and 30 cm depths, and 300 mm for 60 cm depth). Water storage analysis for Cluster 1
436 demonstrated negligible changes under 2% (the measurement accuracy of TDR) in soil moisture
437 that occurred in both the upslope and downslope areas. Rainfall impacts to Cluster 2 can be
438 classified as an intermediate category because both clusters introduced remarkable storage changes
439 (mm) in the downslope area. Significant changes in water storage were observed for Clusters 3, 4,
440 and 5, regardless of the quantity of rainfall. Substantial increases in storage change at a depth of
441 60 cm in the downslope area indicated the generation of subsurface stormflow for Clusters 3, 4,
442 and 5. The main difference between Clusters 3, 4, and 5 was in terms of whether the subsurface
443 lateral flow was generated in the upslope area. Clusters 3 and 5 could be characterized by high
444 rainfall and high ASM, which resulted in subsurface lateral flow in both the upslope and downslope
445 areas. The soil moisture changes and storage for cluster 4 indicated an apparent decreasing trend
446 in the depth profile in the upslope area. The storage changes and soil moisture difference indices
447 at depths of 10 and 30 cm in the upslope area for Cluster 4 were greater than those for Cluster 3
448 due to higher AMO, DUR, and INT. However, the storage change at a depth of 60 cm in the
449 upslope for Cluster 4 was smaller than that of Cluster 3, which could be explained by the lower
450 infiltration under comparatively dry ASM conditions (Zhu et al., 2014; Mei et al., 2018; He et al.,

451 2020). The machine learning algorithm (SOM) can be considered a useful analysis platform not
452 only for elucidating soil moisture response patterns in conjunction with rainfall and ASM (Fig. 7),
453 but also for an effective characterization of soil water storage changes at different locations and
454 depths (Table 2).

메모 포함[오전8]: Response for reveiwer 2's comment "I think the questions which the authors are asking were not directly answered. "

456 4.2 Configuration of hydrological processes

457 The application of SOM, an unsupervised machine learning algorithm, to the dataset provided an
458 integrated assessment for the evaluation and characterization of hydrologic events. The recharge
459 patterns of water storage for the soil layers of the hillslope were characterized by several distinct
460 clusters. The distinct distribution of characteristics of soil moisture responses could be explained
461 by the different combinations of drivers (rainfall and ASM) and hydrological processes (vertical
462 flow, surface, and subsurface lateral flows) for each cluster. The hillslope hydrological flow path
463 was characterized by comparing the component planes between UP10 and UP30 or UP60, and
464 other combinations of soil moisture component planes, such as those of DO10 and DO30 or DO60
465 regarding SDP2P and VAR.

466 The rainfall events can be classified into three distinct categories, which depend on the
467 rainfall characteristics, and five refined clusters as follows: insignificant events for Cluster 1,
468 intermediate events for Cluster 2, and significant events for Clusters 3, 4, and 5 (Table 3). Further
469 classification of significant events indicated that the effects of antecedent moisture conditions and
470 AMO were critical for delineating Clusters 3, 4, and 5. The generation of hydrological processes
471 based on significant soil moisture changes over 2% and increasing patterns of SDP2P (0.11 for 10
472 cm, 0.18 for 30 cm, and 0.22 for 60 cm, respectively) at greater depths was the threshold feature
473 between the insignificant and intermediate events. The primary difference between the

474 intermediate and significant events was deemed the significant response in both the upslope and
475 downslope areas and the substantial development of interface flow between the bedrock and soil
476 layer in the downslope area. This indicated that the lateral flow along boundaries (subsurface and
477 surface) was stronger than that at intermediate depths, and the downslope lateral flow tended to be
478 generated through boundaries either along the surfaces or bedrock. Furthermore, ASM was
479 substantially higher for Clusters 3 and 5 than that for Cluster 4, and the SDP2D in Clusters 3 and
480 5 were lower for all points than those for Cluster 4. This can be explained by the development of
481 preferential pipe flow, which is more common at greater depths under comparatively wet
482 conditions (Lai et al., 2016; Uber et al., 2018; Uchida et al., 2001; Wienhöfer and Zehe, 2014).
483 Low variation and soil moisture changes in UP60 for Cluster 4 indicated that low antecedent
484 moisture conditions could limit the generation of lateral flow in the upslope area, and that of
485 Cluster 3 could be explained by even fewer rainfall events in Cluster 3 than those in Cluster 4, and
486 these were sufficient to activate subsurface lateral flow in the upslope. Extreme rainfall events
487 were mainly associated with Cluster 5. Lateral storm flow likely occurred in both the upslope and
488 downslope areas of Cluster 5. Effective drainage during extreme events seems to be strongly
489 associated with lateral flow generation along the two boundaries in the soil media (i.e., surface and
490 bedrock) (Angermann et al., 2017; Freer et al., 2004; Haga et al., 2005; Kim, 2009; Uchida et al.,
491 2001; Wienhöfer and Zehe., 2014). The impact of extreme rainfall conditions dominates other
492 controls (e.g., land cover and topography) regarding hillslope runoff generation (Feng and Liu,
493 2015).

494 As presented in Table 3, delineated clusters of hydrologic events can be considered to
495 distinctly explain the combinations of hydrological processes such as vertical and lateral flows
496 (either surface and subsurface boundaries) between the upslope and downslope directions. Events

메모 포함[오전9]: Response to reviewer 2's comment as "Perhaps the questions can be better elaborated in the discussions and reflect on the conclusions."

497 from Cluster 1 were insignificant in terms of the hydrologic response, and the primary driver of
498 Cluster 2 was rainfall that partially affected soil water storage (downslope). While the bedrock
499 topography was important for Clusters 3, 4, and 5, the surface topography played an important role
500 for Cluster 5.

메모 포함[오전10]: Response to reviewer 2's comment as "Can the authors perhaps provide a more physical understanding of the clusters?"

501 Several studies have been conducted to model the behavior of hillslope hydrology (Fan et
502 al., 2019; Loritz et al., 2017). The SOM analysis for a large dataset showed an apparent distinct
503 pattern in soil moisture response and flow path generation between upslope and downslope areas
504 depending on antecedent soil moisture and rainfall conditions. This suggests that the performance
505 of the model can be improved as the storage structure of the model (fast and slow reservoirs) (Gao
506 et al., 2014; Gharari et al. 2015) is further classified into upslope and downslope categories. The
507 appearance of Cluster 4 (Table 3) demonstrates nonlinear behaviors in the hydrologic response,
508 which can be explained by the apparent role of macropore flow even under low soil moisture
509 conditions (Beven and Germann, 2013; Nimmo, 2012). The implementation of bypass flow under
510 low ASM and high rainfall conditions into the model structure can help improve the modeling of
511 soil water travel time (Kim, 2014). Further elaboration in modeling to represent dual lateral
512 boundary flows in Cluster 5 can be useful to address multiple drain flow pathways under extreme
513 rainfall conditions.

메모 포함[오전11]: Response to reviewer 2's comment as "I would like to encourage the authors to bring their study into wider hydrological modeling efforts. What is the message of the results for the hillslope hydrology at a larger scale?"

515 5 Conclusion

516 Rainfall characteristics and responses of soil moisture at the hillslope scale were explored by
517 applying SOM to a dataset comprising information on a considerable number of hydrologic events.
518 Hydrologic events were characterized by using rainfall and soil moisture data collected over a

519 period of ten years from a steep hillside. Based on a delineated dendrogram, the classification of
520 neurons into five clusters provided meaningful interpretations for understanding hydrologic events.
521 The nonlinear relationships between the hydrologic variables were effectively expressed in the 2D
522 SOM presentations of the variables. The apparent relationship between ASM and peak time
523 variation indicates that the hydrologic response is more feasible under comparatively wet
524 conditions. Water storage analysis for each event from different clusters suggests that spatially
525 different combinations of soil moisture difference index can be attributed to the identified
526 hydrologic response for each cluster. Combinations of upslope and downslope spatial patterns of
527 hillslope hydrological processes, vertical flow, and lateral flow along surface or subsurface
528 boundaries were attributable for the distinctions observed between the event clusters. Depending
529 on the rainfall and ASM conditions delineated from each cluster, the spatial distribution of
530 hydrological processes can be predicted to be useful for obtaining systematic insights into the
531 hillslope hydrological response. The SOM can be considered a useful analysis tool not only to
532 understand the different soil moisture response patterns between the upslope and downslope areas
533 but also to configure particular hydrological processes for delineated clusters. The meta-heuristic
534 classification of hydrologic events provides a better understanding of hydrologic conditions and
535 their drivers, which is vital for designing a process-based hillslope hydrology model.

536

537

538

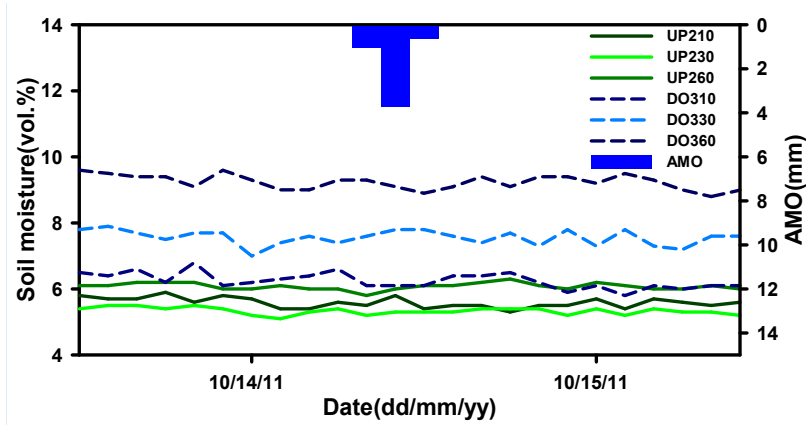
539

540

메모 포함[오전12]: Response to a comment from reviewer 2 as "Perhaps the questions can be better elaborated in the discussions and reflect on the conclusions."

541 Appendix. Exemplary events for Clusters 1 to 5

542

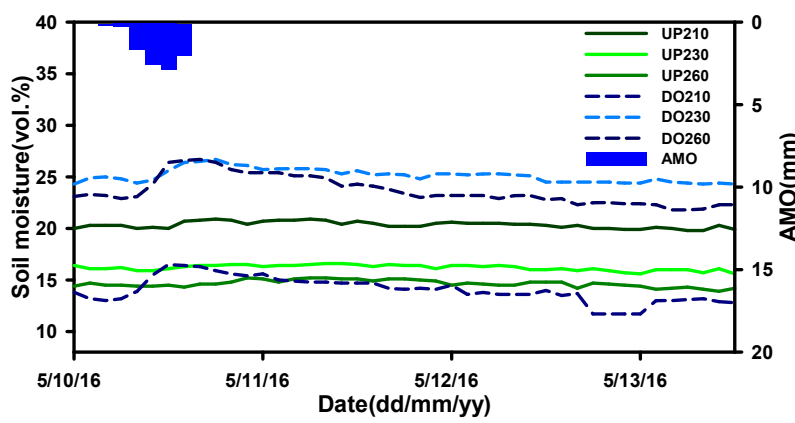


543

Figure A1. Exemplary event (rainfall and soil moisture) for Cluster 1

544

545

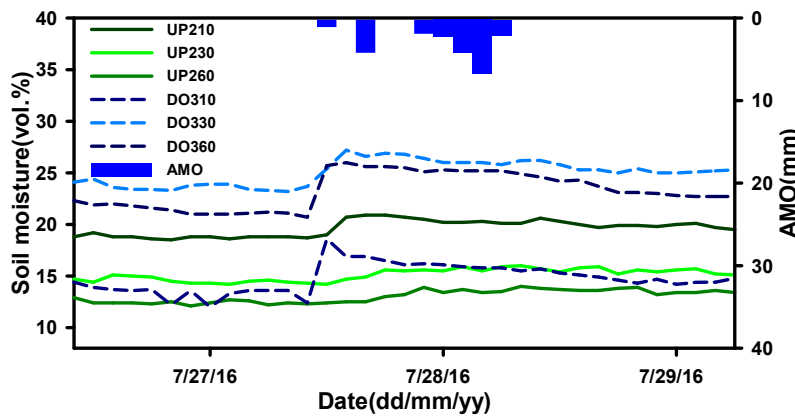


546

Figure A2. Exemplary event (rainfall and soil moisture) for Cluster 2

547

548

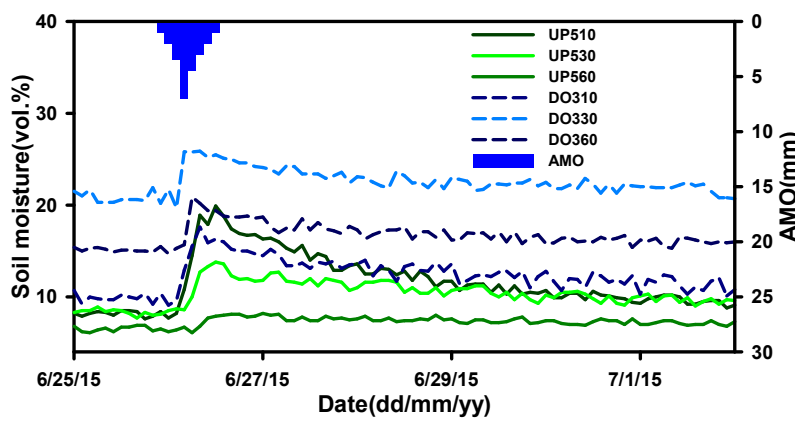


549

550

551

Figure A3. Exemplary event (rainfall and soil moisture) for Cluster 3



552

553

554

Figure A4. Exemplary event (rainfall and soil moisture) for Cluster 4

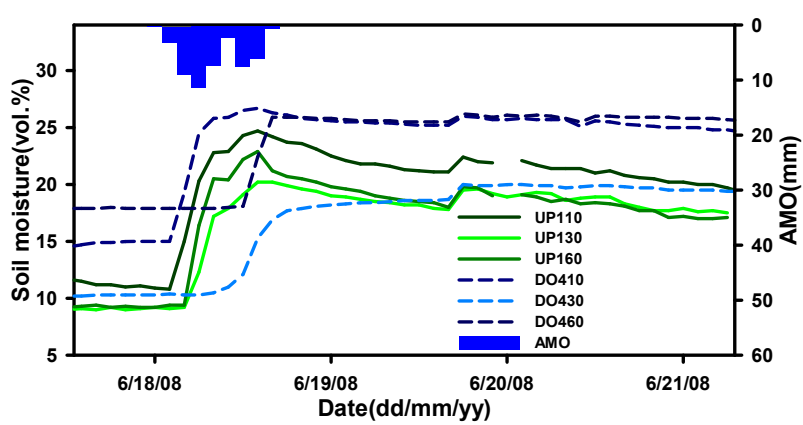


Figure A5. Exemplary event (rainfall and soil moisture) for Cluster 5

메모 포함[오전13]: Revised figures for centroid of each cluster

555

556

557

558 **Code and Data Availability**

559 The code will be available through the repository <https://www.re3data.org/> once the paper is
 560 accepted. The data have been uploaded as supplementary materials.

561

562 **Author contribution**

563 Eunhyung Lee, Sanghyun Kim, and several former graduate students collected data for the study
 564 area. Lee developed the model code and performed simulations. Sanghyun Kim drafted and revised
 565 the manuscript. Both authors have approved the final version of the manuscript.

566

567 **Competing interests**

568 The authors declare that they have no conflict of interest

569

570 **Acknowledgments**

571 This study was financially supported by the Basic Research Program (2016R1D1A1B02008137)
572 of the National Science Foundation of the Republic of Korea.

573

574 **References**

- 575 Adeloje, A. J., Rustum, R., and Kariyama, I.D.: Kohonen self-organizing map estimator for the
576 reference crop evapotranspiration, *Water Resources Research*, 47,
577 10.1029/2011WR010690, 2011.
- 578 Ahmad, S., Kalra, A., and Stephen, H.: Estimation soil moisture using remote sensing data: A
579 machine learning approach, *Advances in Water Resources*, 33, 69-80,
580 10.1016/j.advwatres.2009.10.008, 2010.
- 581 Albertson, J. D., and Kiely, G.: On the structure of soil moisture time series in the context of land
582 surface models, *Journal of Hydrology*, 243, 101-119, 10.1016/S0022-1694(00)00405-4,
583 2001.
- 584 Ali, M., Fiori, A., and Bellotti, G.: Analysis of the nonlinear storage-discharge relation for
585 hillslopes through 2D numerical modelling, *Hydrological Processes*, 27, 2683-2690,
586 10.1002/hyp.9397, 2013.
- 587 Angermann, L., Jackish, C., Allroggen, N., Sprenger, M., Zehe, E., Tronicke, J., Weiler, M., and
588 Blume, T.: Form and function in hillslope hydrology: characterization of subsurface flow
589 based on response observations, *Hydrology and Earth System Sciences*, 21, 3727-3748,
590 10.5194/hess-21-3727-2017, 2017.
- 591 Bachmair, S., Weiler, M., and Troch, P. A.: Intercomparing hillslope hydrological dynamics:
592 Spatio-temporal variability and vegetation cover effects, *Water Resources Research*, 48,
593 W05537, 10.1029/2011WR011196, 2012.
- 594 Baroni, G., Ortuni, B., Facchi, A., and Gandolfi, C.: The role of vegetation and soil properties on
595 the spatio-temporal variability of the surface soil moisture in a maize-cropped field, *Journal*
596 *of Hydrology*, 489, 148-159, 10.1016/j.jhydrol.2013.03.007, 2013.
- 597 Beven, K., Germann, P., Macropores and water flow in soils revisited. *Water Resources Research*
598 49, 3071-3092, 10.1002/wrcr.20156. 2013.
- 599 Carranza, C., Nolet, C., Pejij, M., Ploeg, and van der Ploeg, M.: Root zone soil moisture estimation
600 with random forest, *Journal of Hydrology*, 593, 125840, 10.1016/j.jhydrol.2020.125840,
601 2021.
- 602 Casper, M.C., Grigoryan, G., Gronz, O., Gutjahr, O., Heinemann, G., Ley R., and Rock, A.:
603 Analysis of projected hydrological behavior of catchments based on signature indices,
604 *Hydrology and Earth System Sciences*, 16, 409-421, 10.5194/hess-16-409-2012, 2012.

605 Castillo, V.M., Gomez-Plaza, A., and Martinez-Mena, M.: The role of antecedent soil water
606 content in the runoff response of semiarid catchments: a simulation approach, *Journal of*
607 *Hydrology*, 284, 114-130, 10.1016/S0022-1694(03)00264-6, 2003.

608 Chen, I.T., Chang, L.C., and Chang, F.J.: Exploring the spatio-temporal interrelation between
609 groundwater and surface water by using the self-organizing maps, *Journal of Hydrology*,
610 556, 131-142, 10.1016/j.jhydrol.2017.10.015, 2018.

611 Crow, W.T., and Ryu, D.: A new data assimilation approach for improving runoff prediction using
612 remotely-sensed soil moisture retrievals, *Hydrology and Earth System Sciences*, 13, 1-16,
613 10.5194/hess-13-1-2009, 2009.

614 Curtu, R., Mantilla, R., Fonley, M., Cunha, L.K., Small, S.J., Jay, L.O., and Krajewski, W.F.: An
615 integral-balance nonlinear model to simulate changes in soil moisture, groundwater and
616 surface runoff dynamics at the hillslope scale, *Advances in Water Resources*, 71, 125-139,
617 10.1016/j.advwatres.2014.06.003, 2014.

618 di Prinzio, M., Cstellarin, A., and Toth, E.: Data-driven catchment classification: application to
619 the pub problem, *Hydrology and Earth System Sciences*, 15, 1921-1935, 10.5194/hess-15-
620 1921-2011, 2011.

621 Farsadnia, F., Kamrood, M. R., Nia, A. M., Modarres, R., Bray, M. T., Han, D., and Sadatinejad,
622 J.: Identification of homogeneous regions for regionalization of watersheds by two-level
623 self-organizing feature maps, *Journal of Hydrology*, 509, 387-397,
624 10.1016/j.jhydrol.2013.11.050, 2014.

625 Fan, Y., Clark, M., Lawrence, D. M., Swenson, S., Band, L. E., Brantley, S. L., Brooks, P. D.,
626 Dietrich, W. E., Flores, A., Grant, G., Kirchner, J. W., Mackay, D. S., McDonnell, J. J.,
627 Milly, P.C.D., Sullivan, P. L., Tague, C., Ajami, H., Chaney, N., Hartmann, A., Hazenberg,
628 P., McNamara, J., Pelletier, J., Perket, J., Rouholahnejad-Freund, E., Wagener, T., Zeng,
629 X., Beighley, E., Buzan, J., Huang, M., Livneh, B., Mohanty, B. P., Nijssen, B., Safeeq,
630 M., Shen, C., Verseveld, W. van, Volk, J., Yamazaki, D.: Hillslope hydrology in global
631 change research and earth system modeling, *Water Resources Research*, 55, 1737-1772,
632 10.1029/2018WR023903, 2019.

633 Feng, H., and Liu, Y.: Combined effects of precipitation and air temperature on soil moisture in
634 different land covers in a humid basin, *Journal of Hydrology*, 531, 1129-1140,
635 10.1016/j.jhydrol.2015.11.016, 2015.

636 Freer, J., McDonnell, J., Beven, K., Peters, N. E., Burns, D. A., Hooper, R. P., Aulenbach, B., and
637 Kendall, C.: The role of bedrock topography on subsurface storm flow, *Water Resources*
638 *Research*, 38(12), W1269, 10.1029/2001WR000872, 2004.

639 Gao, H., Hrachowitz, M., Fenicia, F., Gharari, S., Savenije, H.H.G.: Testing the realism of a
640 topography-driven model (FLEX-Topo) in the nested catchment of the Upper Heihe, China.
641 *Hydrology and Earth System Sciences*, 18, 1895-1915, 10.5194/hess-18-1895-2014. 2014.

642 Gharari, S., Hrachowitz, M., Fenicia, F., Gao, H., Savenije, H. H. G.: Using expert knowledge to
643 increase realism in environmental system models can dramatically reduce the need for
644 calibration. *Hydrology Earth System Sciences*, 18, 4839-4859, 10.5194/hess-18-4839-
645 2014. 2015

- 646 Gwak, Y., Kim, S.: Factors affecting soil moisture spatial variability for a humid forest hillslope,
647 *Hydrological Processes*, 31, 431-445, 10.1002/hyp.11039, 2016.
- 648 Haga, H., Matsumoto, Y., Matsutani, J., Fujita, M., Nishida, K., and Sakamoto, Y.: Flow paths,
649 rainfall properties, and antecedent soil moisture controlling lags to peak discharge in a
650 granitic unchanneled catchment, *Water Resources Research*, 41, W12410,
651 10.1029/2005WR004236, 2005.
- 652 Hardie, M.A., Cotching, W.E., Doyle, R.B., Holz, G., Lisson, S., and Mattern, K.: Effect of
653 antecedent soil moisture on preferential flow in a texture-contrast soil, *Journal of*
654 *Hydrology*, 398, 191-201, 10.1016/j.jhydrol.2010.12.008, 2011.
- 655 He, Z., Jia, G., Liu, Z., Zhang, Z., Yu, X., and Xiao, P.: Field studies on the influence of rainfall
656 intensity, vegetation cover and slope length on soil moisture infiltration on typical
657 watersheds of the Loess Plateau, China, *Hydrological Processes*, 34, 4904-4919,
658 10.1002/hyp.13892, 2020.
- 659 He, Z., Zhao, W., Liu, H., and Chang, X.: The response of soil moisture to rainfall event size in
660 subalpine grassland and meadows in a semi-arid mountain range: a case study in
661 northwestern China's Qilian Mountains, *Journal of Hydrology*, 420-421, 183-190,
662 10.1016/j.jhydrol.2011.11.056, 2012.
- 663 Heisler-White, J. L., Knapp, A. K., and Kelly, E. F.: Increasing precipitation event size increases
664 aboveground net primary productivity in a semi-arid grassland, *Oecologia*, 158, 129-140,
665 10.1007/s00442-008-1116-9, 2008.
- 666 Herbst, M., Gupta, H.V., and Casper, M.C.: Mapping model behavior using self-organizing maps,
667 *Hydrology and Earth System Sciences*, 13, 395-409, 10.5194/hess-13-395-2009, 2009.
- 668 Iglesias, F., and Kastner, W.: Analysis of similarity measures in times series clustering for the
669 discovery of building energy patterns, *Energies*, 6, 579-597, 10.3390/en6020579, 2013.
- 670 Ismail, S., Shabri, A., and Samsudin, R.: A hybrid model of self organizing maps and least square
671 support vector machine for river flow forecasting, *Hydrology and Earth System Sciences*,
672 16, 4417-443, 10.5194/hess-16-4417-2012, 2012.
- 673 Kim, S.: Characterization of soil moisture responses on a hillslope to sequential rainfall events
674 during late autumn and spring, *Water Resources Research*, 45, W09425,
675 10.1029/2008WR007239, 2009.
- 676 Kim, S.: Hydrometric Transit Times along Transects on a Steep Hillslope, *Water Resources*
677 *Research*, 50, 7267-7284, 10.1002/2013WR014746, 2014.
- 678 Kohonen, T.: *Self-Organizing Maps*, third ed., Springer, Berlin, 2001.
- 679 Lai, X., Liao, K., Feng, H., and Zhu, Q.: Responses of soil water percolation to dynamic
680 interactions among rainfall, antecedent moisture and season in forest site, *Journal of*
681 *Hydrology*, 540, 565-573, 10.1016/j.jhydrol.2016.06.038, 2016.
- 682 Lee, E. and Kim, S.: Pattern similarity based soil moisture analysis for three seasons on a steep
683 hillslope, *Journal of Hydrology*, 551, 484-494, 10.1016/j.jhydrol.2017.06.028, 2017.

684 Lee E., and Kim, S.: Characterization of runoff generation in a mountainous hillslope according
685 to multiple threshold behavior and hysteretic loop features, *Journal of Hydrology*, 590,
686 125534, 10.1016/j.jhydrol.2020.125534, 2020.

687 Ley, R., Casper, M. C., Hellebrand, H., and Merz, R.: Catchment classification by runoff behavior
688 with self-organizing maps (SOM), *Hydrology and Earth System Sciences*, 15, 2947-2962,
689 10.5194/hess-15-2947-2011, 2011.

690 Li, X. Y., Zhang, S. Y., Peng, H. Y., Hu, X., and Ma, Y. J.: Soil water and temperature dynamics
691 in shrub-encroached grasslands and climatic implications: Results from inner Mongolia
692 steppe ecosystem of north China, *Agricultural and Forest Meteorology*, 171, 20-30,
693 10.1016/j.agriformet.2012.11.001, 2013.

694 Liang, W. L., Kosugi, K., and Mizuyama, T.: Soil water dynamics around a tree on a hillslope with
695 or without rainwater supplied by stemflow, *Water Resources Research*, 47, W02541,
696 10.1029/2010WR009856, 2011.

697 Liao, K., Zhou, Z., Lai, X., Zhu, Q., and Feng, H.: Evaluation of different approaches for
698 identifying optimal sites to predict mean hillslope soil moisture content, *Journal of*
699 *Hydrology*, 547, 10-20, 10.1016/j.jhydrol.2017.01.043, 2017.

700 Loritz, R., Sibylle, K.H., Conrad, J., Niklas, A., Schaik, L. van, Wienhöfer, J., Zehe, E.; Picturing
701 and modeling catchments by representative hillslopes, *Hydrology and Earth System*
702 *Sciences*, 21, 1225-1249, 10.5194/hess-21-1225-2017, 2017.

703 López García, H., and Machón González, I.: Self-organizing map and clustering for wastewater
704 treatment monitoring, *Engineering Application of Artificial Intelligence*, 17, 215-225,
705 10.1016/j.engappai.2004.03.004, 2004.

706 Lu, N., Godt, J.: Infinite slope stability under steady unsaturated seepage conditions, *Water*
707 *Resources Research*, 44, W11404, 10.1029/2008WR006976, 2008.

708 Mei, X., Zhu, Q., Ma, L., Zhang, D., Wang, Y., and Hao, W.: Effect of stand origin and slope
709 position on infiltration pattern and preferential flow on a Loess hillslope, *Land Degradation*
710 *& Development*, 29, 1353-1365, 10.1002/ldr.2928, 2018.

711 Montero, P., Vilar, J.A.: TSclust: An R package for time series clustering, *Journal of Statistical*
712 *Software*, 62, 1-43, 10.18637/jss.v062.i01, 2014.

713 Nimmo, J. R.: Preferential flow occurs in unsaturated conditions, *Hydrological Processes*, 26, 786-
714 789, 10.1002/hyp.8380, 2012.

715 Park, Y. S., Cereghino, R., Compin, A., and Lek, S.: Applications of artificial neural networks for
716 patterning and predicting aquatic insect species richness in running waters, *Ecological*
717 *Modelling*, 160, 265-280, 10.1016/S0304-3800(02)00258-2, 2003.

718 Penna, D., Borga, M., Norbiato, D., and Fontana, G. D.: Hillslope scale soil moisture variability
719 in a steep alpine terrain, *Journal of Hydrology*, 364, 311-327,
720 10.1016/j.jhydrol.2008.11.009, 2009.

721 Penna, D., Tromp van Meerveld, H. J., Gobbi, A., Borga, M., and Fontana, G. D.: The influence
722 of soil moisture on threshold runoff generation processes in an alpine headwater catchment,
723 *Hydrology and Earth System Sciences*, 15, 689-702, 10.5194/hess-15-689-2011, 2011.

- 724 Ramirez, D. A., Bellot, J., Domingo, F., and Blasco, A.: Can water responses in *stipa tenacissima*
725 L. during the summer season be promoted by non-rainfall water gains in soil? *Plant and*
726 *Soil*, 291, 67-79, 10.1007/s11104-006-9175-3, 2007.
- 727 Reusser, D. E., Blume, T., Schaeferli, B., and Zehe, E.: Analysing the temporal dynamics of model
728 performance for hydrological models, *Hydrology and Earth System Sciences*, 13, 999-
729 1018, 10.5194/hess-13-999-2009, 2009.
- 730 Rodriguez-Iturbe, I., Isham, V., Cox, D. R., Manfreda, S., and Porporato, A.: Space-time modeling
731 of soil moisture: Stochastic rainfall forcing with heterogeneous vegetations, *Water*
732 *Resources Research*, 42, W06D05, 10.1029/2005WR004497, 2006.
- 733 Rosenbaum, U., Bogena, H. R., Herbst, M., Huisman, J. A., Peterson, T. J., Weuthen, A., Western,
734 A. W., and Vereecken, H.: Seasonal and event dynamics of spatial soil moisture patterns
735 at the small catchment scale, *Water Resources Research*, 48, W10544,
736 10.1029/2011WR011518, 2012.
- 737 Saffarpour, S., Western, A.W., Adams, R., and McDonnell, J.J.: Multiple runoff processes and
738 multiple thresholds control agricultural runoff generation, *Hydrology and Earth System*
739 *Sciences*, 20, 4525-4545, 10.5194/hess-20-4525-2016, 2016.
- 740 Shrestha, D.L., Kayastha, N., and Solomatine, D.P.: A novel approach to parameter uncertainty
741 analysis of hydrological models using neural networks, *Hydrology and Earth System*
742 *Sciences*, 13, 1235-1248, 10.5194/hess-13-1235-2009, 2009.
- 743 Srivastava, P.K., Han, D., Ramirez, M.R., and Islam, T.: Machine learning techniques for
744 downscaling smos satellite soil moisture using modis land surface temperature for
745 hydrological application, *Water Resources Management*, 27, 3127-3144, 10.1007/s11269-
746 013-0337-9, 2013.
- 747 Toth, E.: Catchment classification based on characterization of streamflow and precipitation time
748 series, *Hydrology and Earth System Sciences*, 17, 1149-1159, 10.5194/hess-17-1149-2013,
749 2013.
- 750 Tromp van Meerveld, I., and McDonnell, J.J.: Comment to “Spatial correlation of soil moisture in
751 small catchments and its relationship to dominant spatial hydrological processes”, *Journal*
752 *of Hydrology*, 286, 113-134”, *Journal of Hydrology*, 303, 307-312,
753 10.1016/j.jhydrol.2004.09.002, 2005.
- 754 Tramblay, Y., Bouaicha, R., Brocca, L., Dorigo, W., Bouvier, C., Camici, S., and Servat, E.:
755 Estimation of antecedent wetness conditions for flood modelling in northern morocco,
756 *Hydrology and Earth System Sciences*, 16, 4375-4386, 10.5194/hess-16-4375-2012, 2012.
- 757 Uber, M., Vandervaere, J.P., Zin, I., Braud, I., Heistermann, M., Legout, C., Molinie, G., and Nord,
758 G.: How does initial soil moisture influence the hydrological response? A case study from
759 southern france, *Hydrology and Earth System Sciences*, 22, 6127-6146, 10.5194/hess-22-
760 6127-2018, 2018.
- 761 Uchida, T., Kosugi, K., and Mizuyama, T.: Effects of pipeflow on hydrological process and its
762 relations to landslide, a review of pipeflow studies in forested headwater catchments,
763 *Hydrological Processes*, 15, 2151-2174, 10.1002/hyp.281, 2001.

764 Van Arkel, Z., and Kaleita, A. L.: Identifying sampling locations for field-scale soil moisture
765 estimation using K-means clustering, *Water Resources Research*, 50, 7050-7057,
766 10.1002/2013WR015015, 2014.

767 Wang, S., Fu, B., Gao, G., Liu, Y., and Zhou, J.: Responses of soil moisture in different land cover
768 types to rainfall events in a re-vegetation catchment area of the Loess Plateau, China,
769 *Catena*, 101,122-128, 10.1016/j.catena.2012.10.006, 2013.

770 Wang, X. P., Cui, Y., Pan, Y. X., Li, X. R., Yu, Z., and Young, M. H.: Effects of rainfall
771 characteristics on infiltration and redistribution patterns in revegetation-stabilized desert
772 ecosystems, *Journal of Hydrology*, 358, 134-143, 10.1016/j.jhydrol.2008.06.002, 2008.

773 Ward, J. H.: Hierarchical grouping to optimize an objective function, *Journal of the American*
774 *Statistical Association*, 58, 236-244, 1963.

775 Western, A. W., Grayson, R. B., Blöschl, G. Willgoose, G. R., McMahon, T. A.: Observed spatial
776 organization of soil moisture and its relation to terrain indices, *Water Resources Research*,
777 35(3), 797-8110, 10.1029/1998WR900065, 1999.

778 Wienenkamp, I., Huisman, J.A., Bogen, H.R., Lin, H.S., and Vereecken, H.: Spatial and temporal
779 occurrence of preferential flow in a forested headwater catchment, *Journal of Hydrology*,
780 534, 139-149, 10.1016/j.jhydrol.2015.12.050, 2016.

781 Wienhöfer, J., and Zehe, E.: Predicting subsurface stormflow response of a forested hillslope: the
782 role of connected flow paths, *Hydrology and Earth System Sciences*, 18, 121-138,
783 10.5194/hess-18-121-2014, 2014.

784 Wilson, D. J., Western, A. W., and Grayson, R. B.: Identifying and quantifying sources of
785 variability in temporal and spatial soil moisture observations, *Water Resources Research*,
786 40, W02507, 10.1029/2003WR002306, 2004.

787 Zhang, Y., Wei, H., and Nearing M.A.: Effects of antecedent soil moisture on runoff modeling in
788 small semiarid watersheds of southeastern Arizona, *Hydrology and Earth System Sciences*,
789 15, 3171-3179,10.5194/hess-3171-2011, 2011.

790 Zhu, Q., Nie, X. F., Zhou, X. B., Liao, K. H., and Li, H. P.: Soil moisture response to rainfall at
791 different topographic positions along a mixed land-use hillslope, *Catena*, 119, 61-70,
792 10.1016/j.catena.2014.03.010, 2014.

793
794
795
796
797
798
799
800
801

802 Figure Captions (7 Figures)

803
804 **Figure 1:** Location of the Sulmachun watershed in South Korea with hydrologic monitoring
805 (rainfall and evapotranspiration) stations (lower left) and study area with terrain contours,
806 topographic wetness index (TWI), and soil moisture monitoring points (right).

807
808 **Figure 2:** Boxplots illustrating soil moisture responses of P2P and Maximum variation at 10 cm
809 depth (a) (b); those at 30 cm depth (c) and (d); those at 60 cm depth (e) and (f), respectively.
810 Elevations in x-axis are between 260 and 215 m as an order of UP1-UP4-UP2-UP5-UP3-DO1-
811 DO2-DO3-DO4-DO5 shown in Fig. 1.

812
813 **Figure 3:** Box plots illustrating antecedent soil moisture (a), soil moisture difference index (b),
814 and standard deviation of peak time (SDP2P) (c) of 12 time series of soil moistures.

815
816 **Figure 4:** Heat maps depicted for the coefficient of determination (R^2) among combinations of
817 (a) antecedent soil moisture, (b) soil moisture difference index, and (c) standard deviation of
818 peak time.

819
820 **Figure 5:** Structure of (a) dendrogram for five clusters and (b) SOM classifications in 96 neurons
821 through the application of a 16×6 matrix.

822
823 **Figure 6: (a)–(p)** Component planes of variable weightings for rainfall amount (AMO) (a); rainfall
824 duration (DUR) (b); rainfall intensity (INT) (c); antecedent soil moisture (ASM) (d); soil moisture
825 difference indices for the upslope and downslope at depths of 10, 30, and 60 cm (VUP10, VUP30,
826 VUP60, VDO10, VDO30, and VDO60) (e)-(j); standard deviation of peak time for the upslope
827 and downslope at depths of 10, 30, and 60 cm (SUP10, SUP30, SUP60, SDO10, SDO30, and
828 SDO60) (k)-(p).

829
830 **Figure 7:** SDP2Ps with mean AMO and ASM for each cluster (a) soil moisture difference indices
831 with mean DUR and INT for each cluster (b) for total, upslope, and downslope at depths of 10, 30,
832 and 60 cm, and the corresponding depths for upslope and downslope.

833

834

835

836

837

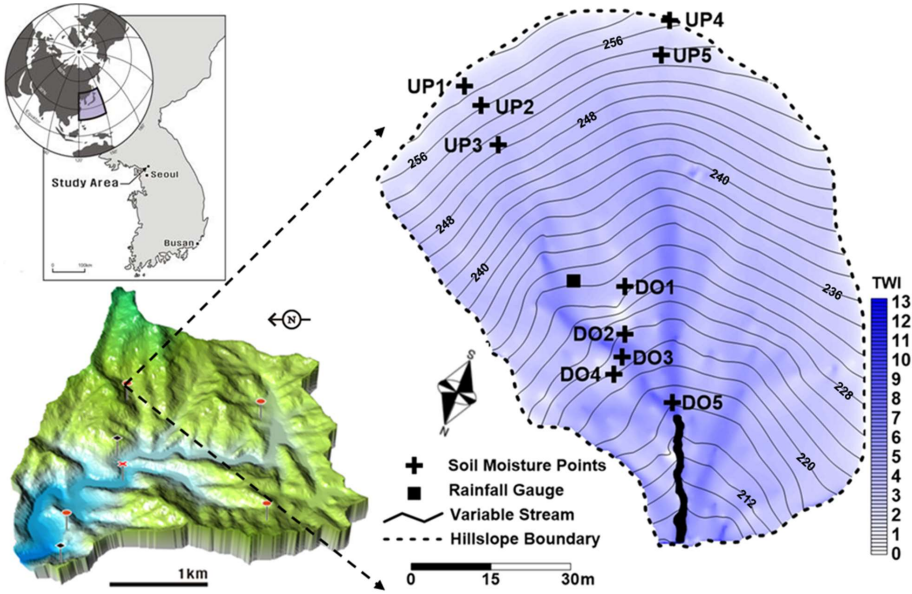
838

839

840

841 **Figure 1.**

842



843

844 **Figure 1:** Location of the Sulmachun watershed in South Korea illustrated with hydrologic
845 monitoring (rainfall and evapotranspiration) stations (lower left) and study area with terrain
846 contours, topographic wetness index (TWI), and soil moisture monitoring points (right).

847

848

849

850

851

852

853

854

855

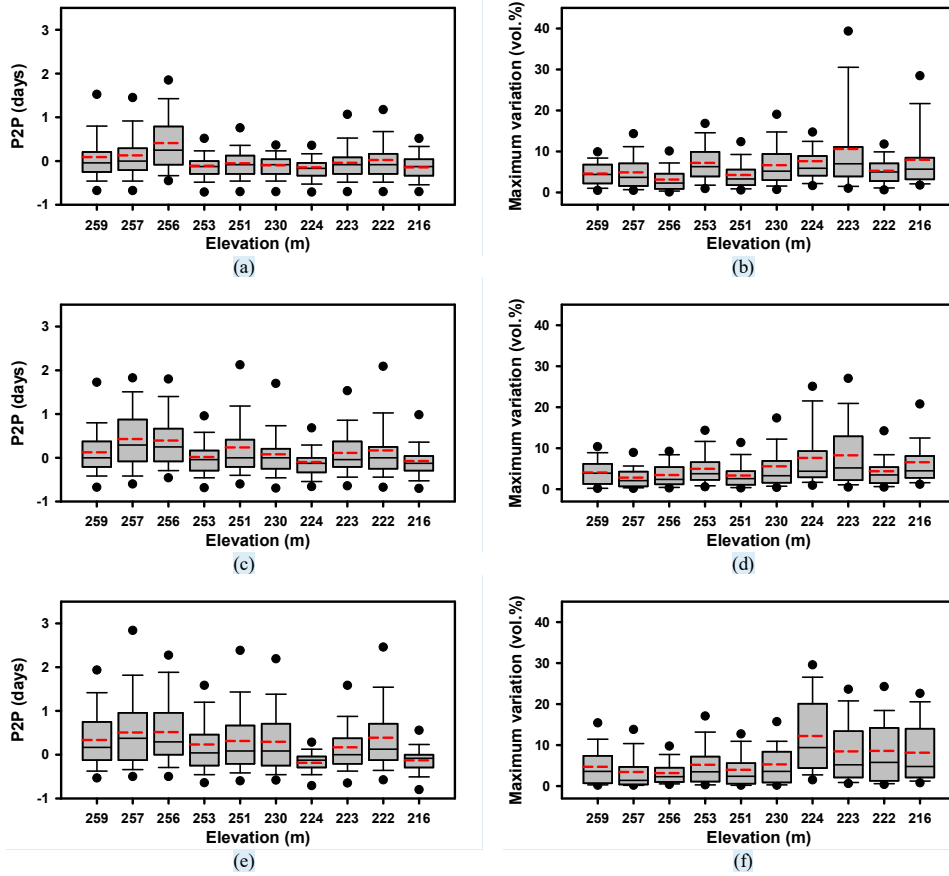
856

857

858

859
860

Figure 2.

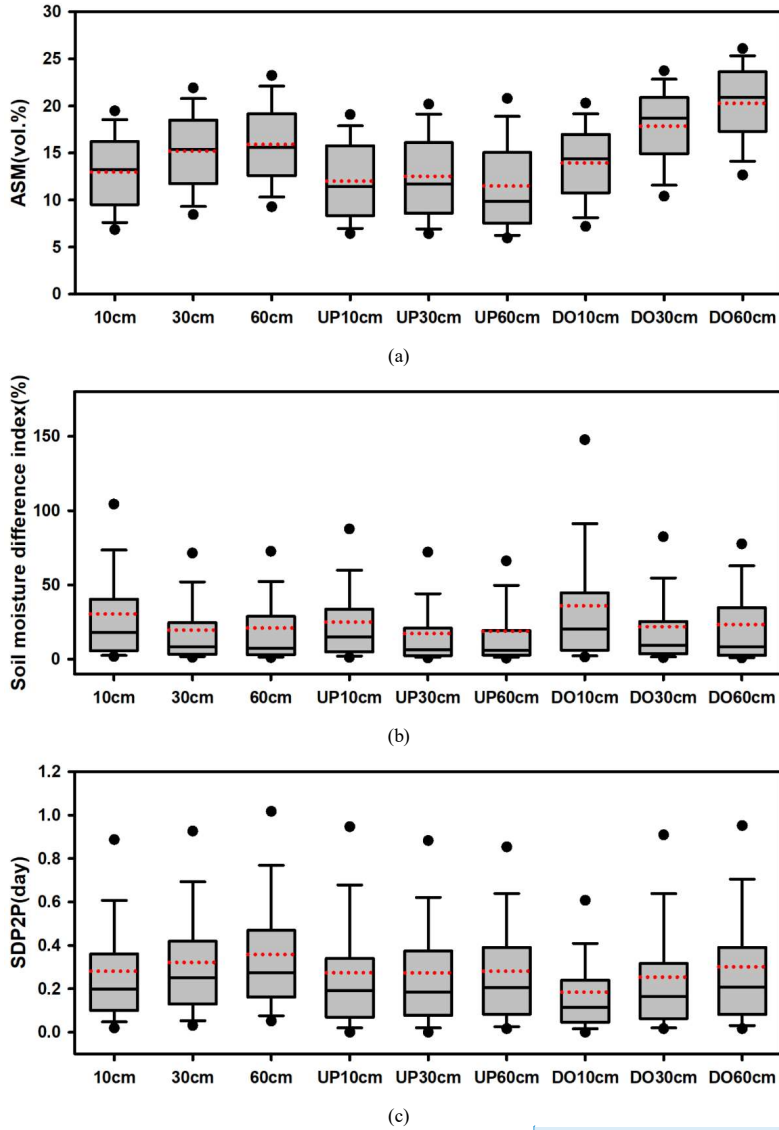


861 **Figure 2:** Boxplots illustrating soil moisture responses of P2P and Maximum variation at 10 cm
862 depth (a) (b); those at 30 cm depth (c) and (d); those at 60 cm depth (e) and (f), respectively.
863 Elevations in x-axis are between 260 and 215 m as an order of UP1-UP4-UP2-UP5-UP3-DO1-
864 DO2-DO3-DO4-DO5 shown in Fig. 1.

865
866
867
868
869

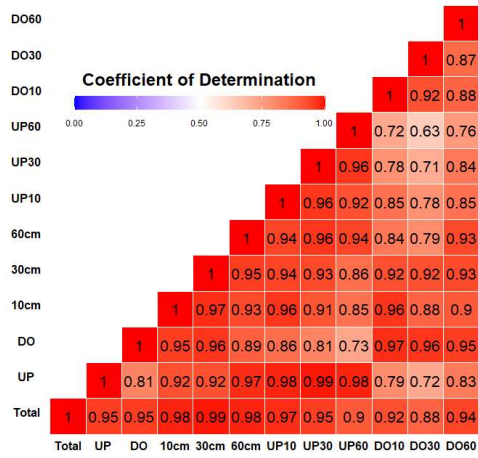
메모 포함[오전14]: Fig. 2 is revised to address final reviewers comment about elevation in x-axis.

870 **Figure 3.**

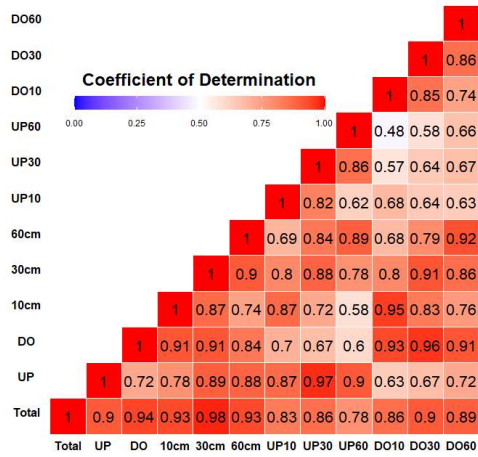


871 **Figure 3:** Box plots illustrating antecedent soil moisture (a), soil moisture difference index (b),
872 and standard deviation of peak time (SDP2P) (c) of 12 time series of soil moistures.
873

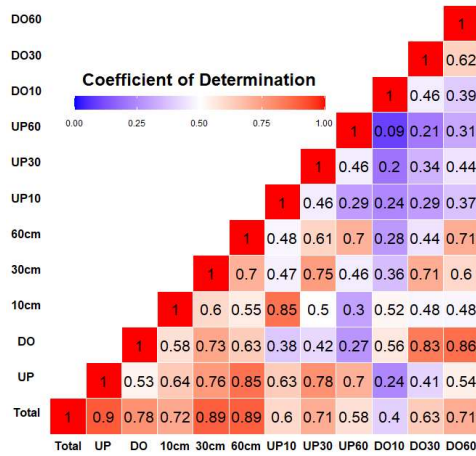
메모 포함[오전15]: Correction for consistent expression



(a)



(b)



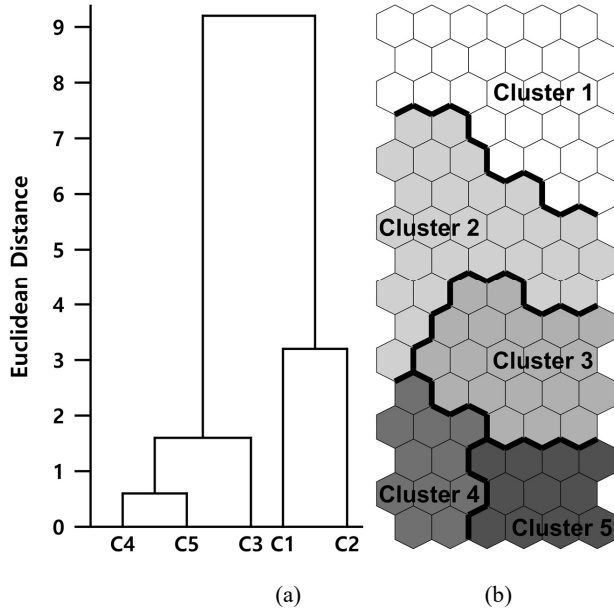
(c)

875 **Figure 4:** Heat maps depicted for the coefficient of determination (R^2) among combinations of (a)
 876 antecedent soil moisture, (b) soil moisture difference index, and (c) standard deviation of peak
 877 time.
 878

메모 포함[오전16]: Fig. 4 is revised to address final reviewer's comment

879
 880
 881
 882
 883
 884
 885
 886
 887
 888
 889
 890
 891
 892
 893
 894

895 **Figure 5.**



896

897

898 **Figure 5:** Structure of (a) dendrogram for five clusters and (b) SOM classifications in 96 neurons
899 through the application of a 16×6 matrix.

900

901

902

903

904

905

906

907

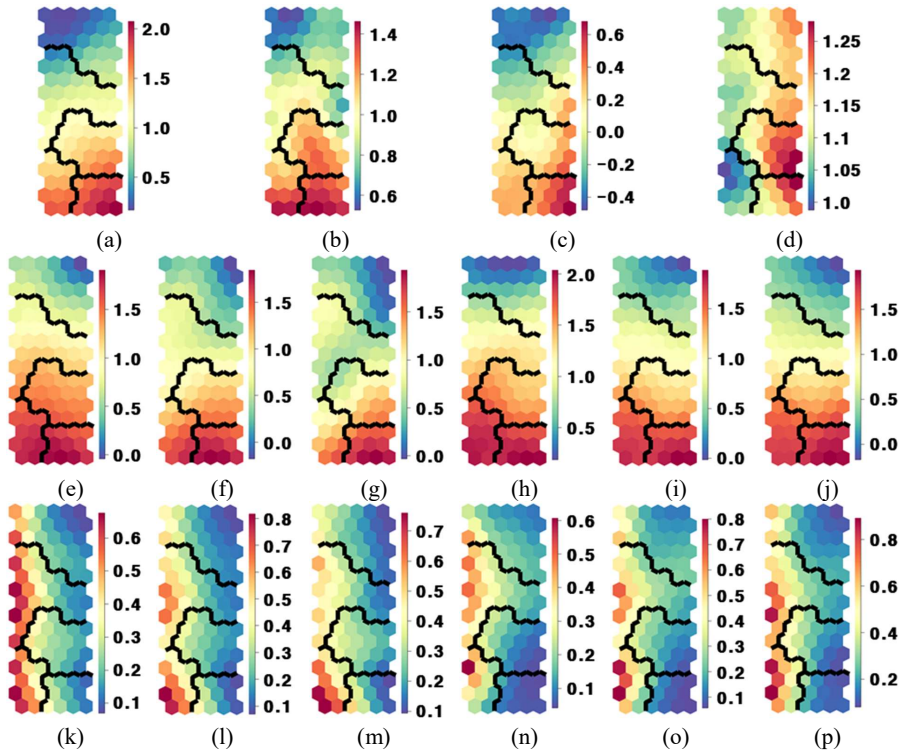
908

909

910

911

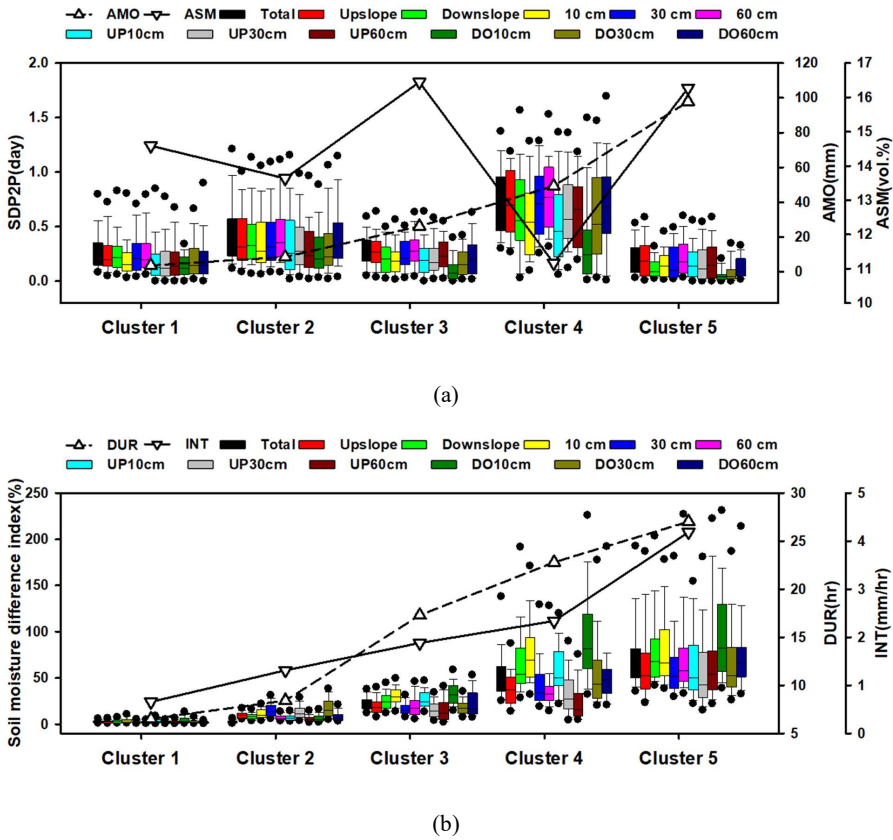
912 **Figure 6.**



913 **Figure 6: (a)–(p)** Component planes of variable weightings for rainfall amount (AMO) (a); rainfall
914 duration (DUR) (b); rainfall intensity (INT) (c); antecedent soil moisture (ASM) (d); volumetric
915 soil moisture difference indices for the upslope and downslope at depths of 10, 30, and 60 cm
916 (VUP10, VUP30, VUP60, VDO10, VDO30, and VDO60) (e)-(j); standard deviation of peak time
917 for the upslope and downslope at depths of 10, 30, and 60 cm (SUP10, SUP30, SUP60, SDO10,
918 SDO30, and SDO60) (k)-(p).
919

920
921
922
923
924
925

926 **Figure 7.**



927 **Figure 7:** SDP2Ps with mean AMO and ASM for each cluster (a) soil moisture difference indices
 928 with mean DUR and INT for each cluster (b) for total, upslope, and downslope at depths of 10, 30,
 929 and 60 cm, and the corresponding depths for upslope and downslope.

메모 포함[오전17]: Correction for consistent expression

930
 931
 932
 933
 934

935

936

937

938 **Table 1.** Arithmetic averages of SOM inputs for rainfall amount (AMO), rainfall duration (DUR),
939 rainfall intensity (INT), antecedent soil moisture for all points (ASMTOT), volumetric soil
940 moisture difference index, and standard deviation of peak-to-peak time (SDP2P).

Variables	Numbers	AMO (mm)	DUR (h)	INT (mm/h)	ASMTOT (vol.%)		
cluster 1	108	3.61	6.50	0.66	14.6		
cluster 2	90	8.45	8.40	1.31	13.6		
cluster 3	75	26.08	17.28	1.88	16.4		
cluster 4	30	49.27	22.80	2.34	11.2		
cluster 5	53	97.80	27.02	4.19	16.3		
Volumetric soil moisture difference index		VUP10	VUP30	VUP60	VDO10	VDO30	VDO60
cluster 1	3.8	2.0	2.5	4.6	2.9	1.9	
cluster 2	13.2	5.7	6.8	17.5	8.6	7.2	
cluster 3	26.9	16.4	16.1	33.4	18.2	22.9	
cluster 4	59.1	33.0	23.4	96.1	56.6	54.8	
cluster 5	66.7	60.8	73.9	100.7	68.6	77.4	
SDP2P		SUP10	SUP30	SUP60	SDO10	SDO30	SDO60
cluster 1	0.21	0.20	0.21	0.16	0.22	0.22	
cluster 2	0.37	0.35	0.33	0.30	0.35	0.42	
cluster 3	0.22	0.22	0.26	0.11	0.18	0.22	
cluster 4	0.56	0.65	0.63	0.36	0.59	0.72	
cluster 5	0.17	0.17	0.20	0.06	0.09	0.12	

메모 포함[오전18]: Correction for consistent expression

메모 포함[오전19]: Correction for consistent expression

941

942

943

944

945

946

947

948

949

950

951 **Table 2.** Soil moisture changes and storage changes for all clusters at depths of 10 cm, 30 cm, and
 952 60 cm, and those recorded for upslope and downslope.

Average	Cluster	10 (cm)	30 (cm)	60 (cm)	Upslope			Downslope		
					10 (cm)	30 (cm)	60 (cm)	10 (cm)	30 (cm)	60 (cm)
Soil moisture change (vol.%)	1	0.5	0.4	0.3	0.4	0.3	0.3	0.6	0.5	0.4
	2	1.9	1.0	1.0	1.5	0.6	0.7	2.3	1.5	1.4
	3	4.5	2.9	3.5	3.7	2.4	2.1	5.2	3.5	5.1
	4	7.4	5.2	4.9	5.3	3.1	2.0	9.8	7.8	9.0
	5	12.0	10.8	13.3	8.9	8.7	10.0	15.4	13.3	16.8
Storage change (mm)	1	1.0	0.8	0.9	0.8	0.6	0.9	1.2	1.0	1.2
	2	3.8	2.0	3.0	3.0	1.2	2.1	4.6	3.0	4.2
	3	9.0	5.8	10.5	7.4	4.8	6.3	10.4	7.0	15.3
	4	14.8	10.4	14.7	10.6	6.2	6.0	19.6	15.6	27.0
	5	24.0	21.6	39.9	17.8	17.4	30.0	30.8	26.6	50.4

953

954

955

956

957

958

959

960

961

962

963

964

965

966

967 **Table 3.** Combinations of flow paths and its hydrologic conditions for all clusters.

Cluster	#	Rainfall impact	Antecedent soil moisture	Upslope		Downslope	
				Vertical flow	Lateral flow SF/SB	Vertical flow	Lateral flow SF/SB
1	108	Insignificant	Mid	No response (under 2 vol.%)		No response (under 2 vol.%)	
2	90	Intermediate	Mid	No response (under 2 vol.%)		Yes	No
3	30		High	Yes	No/Yes	Yes	No/Yes
4	53	Significant	Low	Yes	No/No	Yes	No/Yes
5	75		High	Yes	No/Yes	Yes	Yes/Yes

968 SF: surface; SB: subsurface.

969

970

971

972

973